Development and Analysis of a Thick Cloud Layers Database for Lightning Launch Commit Criteria Improvement

Jacquelyn Ringhausen
NASA Kennedy Space Center
NASA Internship Summer 2020
Mentor: Kristin Smith SI-I1

Abstract

Lightning can pose a potential threat to space launch vehicles. In response to this, rules were created called the Lightning Launch Commit Criteria (LLCC) that help weather personnel evaluate the potential for natural and rocket-triggered lightning. One of the ten LLCC with the least research is called the Thick Cloud Layers rule. To further understand electrification of thick cloud layers and potentially improve the Thick Cloud Layers rule, a database of thick cloud layers that occurred over the Eastern Range was created. This database is then used to create an algorithm for identifying and differentiating thick cloud layers from other cloud types based on radar characteristics, temperature levels in reference to cloud height, and the surface electric field. By analyzing and identifying thick cloud events, this project could help narrow down when thick clouds are occurring and potentially minimize unnecessary launch delays.

Events that caused LLCC violations involving the Thick Cloud Layers rule were analyzed by hand using Level-2 NEXRAD radar data from the National Weather Service WSR-88D radar in Melbourne with the program GR2Analyst. Cases that were found to be isolated and not involved with convection were recorded (date, start/end time, location) in a database. Radar data associated with these cases was collected and gridded using Python radar packages. Once gridded, I calculated and recorded for each radar scan the following radar reflectivity driven parameters within an 11x11 km bin centered on each 1 km^2 grid point: the mean reflectivity colder than 0 degrees Celsius, Maximum Radar Reflectivity (MRR) colder than 0 degrees Celsius, Volume Averaged Height Integrated Radar Reflectivity (VAHIRR), Hydrometeor Identification (HID), the difference between the maximum and mean reflectivity, the cloud depth colder than 0 degrees Celsius, the overall cloud depth, the cloud top, and the cloud bottom. Soundings for each event were used to determine cloud temperature levels, and where the cloud is in relation to the freezing level. Electric field mill data collected over the Eastern Range was used to determine surface electric fields below each cloud. All parameters were analyzed in depth for several thick cloud cases to gain an understanding of typical thick cloud characteristics. Cases of thick clouds and other isolated cloud types were also recorded for training purposes to see if enough differences exist between cloud types to differentiate them with an algorithm. Each case along with its

corresponding characteristics was recorded in a database, and this database was used to compare differing cloud types, as well as train the algorithm to detect thick clouds.

Introduction

Lightning can pose a potential threat to space launch vehicles. In response to this, rules were created called the Lightning Launch Commit Criteria (LLCC) that help weather personnel evaluate the potential for natural and rocket-triggered lightning. In 1969, Apollo XII was launched and was struck twice by triggered lightning (Merceret, 2010). This triggered lightning led to the realization that launch rules needed to be added that included electrified clouds that are not producing natural lightning. One of the ten LLCC related to electrified clouds not currently producing natural lightning is called the Thick Cloud Layers rule (Willett, 2017). To further understand electrification of thick cloud layers and potentially improve the Thick Cloud Layers rule, this project will build a database of thick cloud layers that occurred over the Eastern Range. This database will then be used to create an algorithm for identifying thick cloud layers based on radar characteristics, temperature levels in reference to cloud height, and the surface electric field. By analyzing and identifying thick cloud events, this project could help narrow down when thick clouds are electrified and potentially minimize unnecessary launch delays.

Objectives

1. Identify isolated thick cloud layers from 11 known archived thick cloud layer violation events provided by the 45th Weather Squadron

2. Grid radar data for each event using Python

3. Analyze and record characteristics of thick cloud layers using gridded radar data (vertical integration of contiguous radar reflectivity, maximum reflectivity colder than 0 degrees Celsius, and cloud depth colder than 0 degrees Celsius), soundings (determination of temperature and freezing level in relation to cloud), and electric field mill data (determination of surface electric field)

4. Create and train an algorithm to identify thick clouds using the characteristics collected

6. Test algorithm on collected dataset and calculate skill scores

7. Write a final report detailing the data, methodology, algorithm development, analysis, and results

Data

Electric field mill network

The electric field network used in this study was the KSC field mill network. This network consists of 34 different electric field mills that sense the ambient electric field occurring. In order to get electric field values for each case, data was collected from the KSC Weather data archive. This data is publicly available at the following website:

https://kscwxarchive.ksc.nasa.gov

Once downloaded, the electric field was averaged every 10 seconds to help alleviate noise in the data. Python code was written to do this averaging and load the data in for comparison to other parameters.

Figure 1: Location of Electric field mills surrounding KSC. Taken from: https://kscwxarchive.ksc.nasa.gov/Map

WSR-88D Radar

The radar data used in this analysis was from the WSR-88D KMLB S-Band Radar located in Melbourne, Florida. Radar data for each case is publicly available and downloaded from the NCDC website:

https://www.ncdc.noaa.gov/nexradinv/chooseday.jsp?id=kmlb

Once downloaded, the radar data was gridded using Python PyArt radar packages. We used a 1km by 1km grid spacing, with a 1 km Radius of Influence (ROI). Due to the differing volume coverage patterns and locations of storms in reference to the radar, several cases do have rings in the data where gaps in the elevation angles are present. Using data from a radar with more comprehensive volume coverage patterns (more elevation angles) could help alleviate these rings in future work.

Soundings

Soundings launched from the KSC station were collected for each case day from the Wyoming sounding website:

http://weather.uwyo.edu/upperair/sounding.html

These soundings were used to find the freezing level for each case day and used in the calculation of the Hydrometeor ID (HID). The sounding that occurred closest in time to the event was used. Code was written to load in sounding data and extract freezing level height.

Methodology

This project had two main parts:

1) Analyze thick cloud layer cases in depth

2) Create a logistic regression model to differentiate cloud types

Thick Cloud Layer Analysis

First, events that caused LLCC violations involving the Thick Cloud Layers rule were analyzed by hand using Level-2 NEXRAD radar data from the National Weather Service WSR-88D radar in Melbourne with the program GR2Analyst. Cases that were found to be isolated and not involved with convection were recorded (date, start/end time, location) in a database. Radar data associated with these cases was collected and gridded using Python radar packages. Once gridded, the following radar reflectivity driven parameters were calculated and recorded for each radar scan within an 11x11 km bin centered on each 1 km^2 grid point: the mean reflectivity colder than 0 degrees Celsius, Maximum Radar Reflectivity (MRR) colder than 0 degrees Celsius, Volume Averaged Height Integrated Radar Reflectivity (VAHIRR), Hydrometeor Identification (HID), the difference between the maximum and mean reflectivity, the cloud depth colder than 0 degrees Celsius, the overall cloud depth, the cloud top, and the cloud bottom. Grid points that occurred within 5 nm of an electric field mill were recorded in a database to be used for training the logistic regression model. Soundings for each event were used to determine cloud temperature levels, and where the cloud is in relation to the freezing level. Electric field mill data collected over the Eastern Range was used to determine surface electric fields below each cloud. All parameters were analyzed in depth for 11 thick cloud cases to gain an understanding of typical thick cloud characteristics. Only cases that occurred after the radar had been updated to dual-polarization capabilities were used in this project in order to be able to calculate HID.

Parameters	Description
Maximum Radar Reflectivity (MRR)	The maximum radar reflectivity measurement found within a volume that extends horizontally within an 11 km-by-11 km area and extends vertically from 5 km (approximate altitude of 0 degrees Celsius) to the top of the cloud.
Volume Averaged Height Integrated Radar Reflectivity (VAHIRR)	Average reflectivity in the 11 km-by-11 km column x Average cloud thickness from 0 degrees Celsius
Mean Reflectivity	Mean reflectivity of values above 0 degrees Celsius
Maximum/Mean Reflectivity Difference	Maximum reflectivity subtracted by the average reflectivity
Electric field	Closest electric field mill value in time and spatially within 5 nm
Thickness (above freezing)	Cloud thickness from 0 degrees Celsius
Overall Thickness	Cloud thickness from cloud base to top
Top	Maximum cloud height
Bottom	Minimum cloud height above freezing
Bottom Overall	Minimum cloud height
HID1, HID2, HID3, HID4, HID5, HID6, HID7, HID8, HID9, HID10	Hydrometeor ID as a fraction of the total area for each type

Table 1: Characteristics recorded for each cloud type case and the corresponding definition.

Cases of thick clouds and other isolated cloud types were also recorded for training purposes to see if enough differences exist between cloud types to differentiate them with an algorithm. Only cases with no overlap of other cloud type violations were used in this study. Each case along with its corresponding characteristics was recorded in a database, and this database was used to compare differing cloud types, as well as train the algorithm to detect thick clouds. The four cloud types the model differentiates between are: Thick cloud, Attached Anvil, Detached Anvil, and Cumulus. A list of the violation days used in data collection for the model are shown in Table 2.

	Dates	Training Number	Test Number	Type
Thick Cloud	02/05/2016 06/03/2020 06/04/2020 07/25/2019 12/03/2015 09/07/2014	33794	11361	1
Cumulus	02/23/2016 02/19/2017 07/28/2014 08/07/2013 06/20/2014	21793	7104	2
Attached Anvil	08/05/2014 07/28/2014 07/24/2015 04/13/2015	12979	4256	3
Detached Anvil	07/24/2019 08/05/2014 08/07/2013	23998	8020	0

Table 2: Cases with isolated cloud types used in training and testing of multinomial logistic regression along with the number of each cloud type.

Multinomial Logistic Regression

A logistic regression is a statistical method for analyzing a dataset in which there are one or more independent variables that correlate to an outcome. For this dataset, there are 20 different characteristics (independent variables) used to determine a classification of four different cloud types (dependent variable). The data is split into a training dataset and test dataset. The training dataset is used to train the model in differentiating cloud type, while the test dataset is used to test the model performance after being trained. For this study we used 75% of the data for training and 25% for testing. The multinomial logistic regression model was written in Python. Skill scores are calculated to determine how well the algorithm performs. All of the data collected is combined into a database that can be updated with future cases outside of the scope of the project. The creation of this database ultimately will increase confidence in the statistical significance of the algorithm's ability to detect thick clouds that have the potential to trigger lightning when passed through by a launch vehicle.

Results

Thick Cloud layer cases

In this section we will analyze a few of the thick cloud cases in depth. Images of all 11 thick cloud cases were created and are available, but not included in this report in their entirety. The three chosen cases are meant to showcase the variability in thick cloud cases, as well as their shared characteristics.

<u>06/04/2020:</u>

Starting with the Constant Altitude Plan Position Indicators (CAPPIs), the thick cloud layers on this case day are quite thick in the horizontal and the vertical, with reflectivity values above 20 showing up at both 4 and 7 km heights (Figure 2). In general, reflectivity values are quite cohesive, with little variation in the horizontal. When viewing the RHI plots, we can see more clearly the vertical extent of this thick cloud, with reflectivity ranging from the surface to 11 km (Figure 3). The HID for this thick cloud is a mixture of aggregates, vertical ice, and ice crystals, with aggregates occurring closer to the freezing level and ice crystals further aloft. This is understandable since aggregates are heavier than ice crystals, and thus ice crystals are able to be lofted higher. Also, from -10 to -20 degrees C is where aggregate growth is most efficient, and this is where the aggregates are located in this thick cloud. Electric field values are quite weak, with values of ~150 V/m occurring (Figure 4). This value falls within the fair-weather field values, i.e. The value of the ambient electric field when no clouds are occurring. The maximum MRR appears to occur where relatively weaker electric fields are occurring, while weaker MRR is occurring near the relatively stronger fields (although all the electric field values were weak regardless).

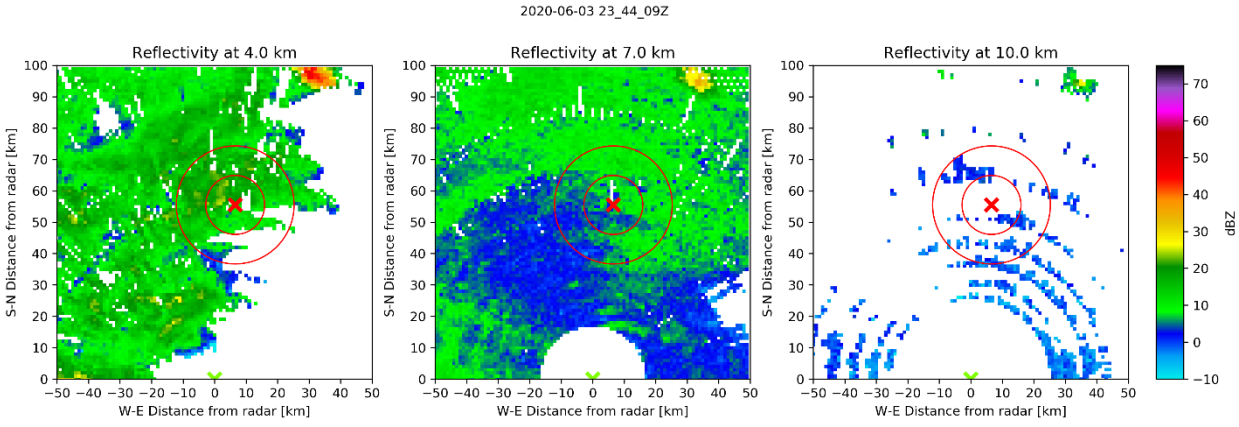

Figure 2: 4km, 7km, and 10km CAPPIs of reflectivity for a thick cloud layer from 6/4/2020. Red 'x' represents the approximate location of KSC, with 5 nm and 10 nm rings.

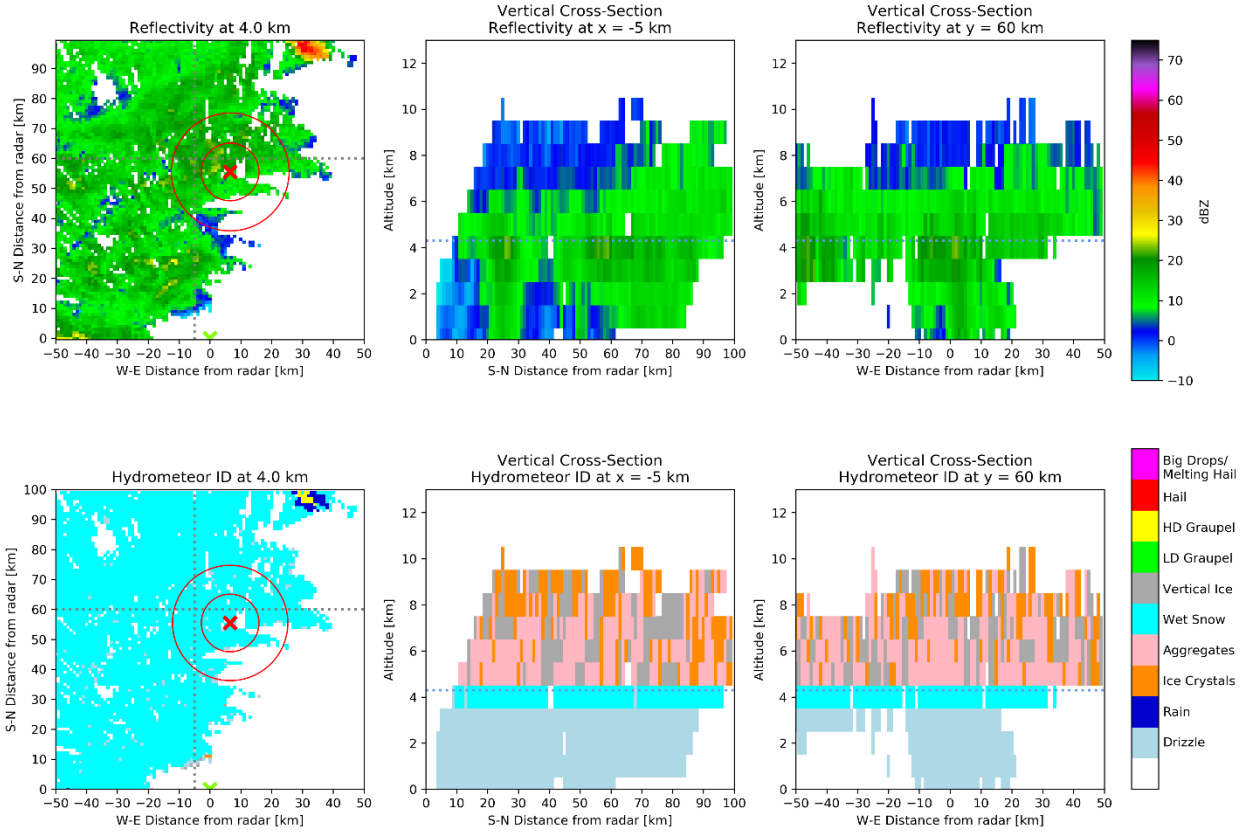

Figure 3: 4km CAPPI and RHIs of reflectivity and HID for a thick cloud layer from 6/4/2020. Cross section location is marked by dotted lines on CAPPI and radar location is marked by the green arrow.

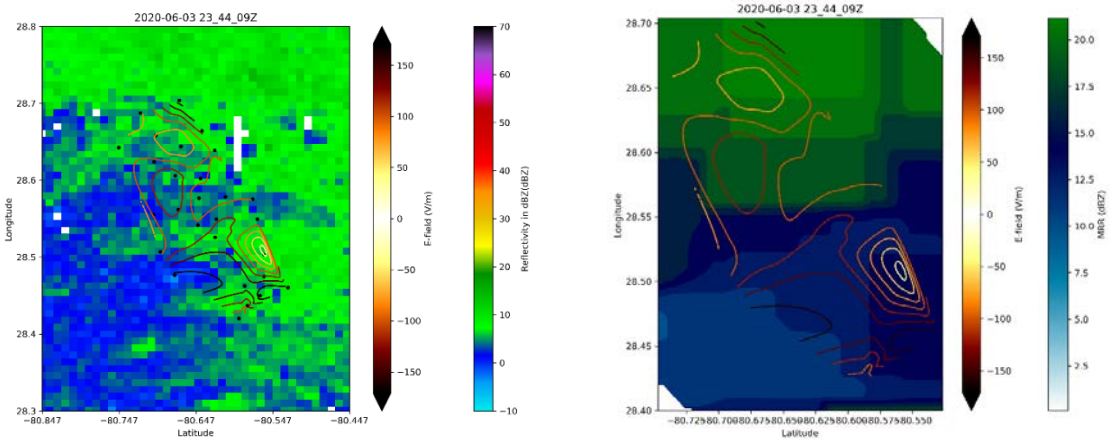

Figure 4: Electric field contours overplotted on reflectivity CAPPI (left), and MRR (right), for a thick cloud layer from 6/4/2020.

07/25/2019:

The second case day was less expansive with a small area of thick cloud passing over the KSC area. This cloud had reflectivity values of less than 20 dBZ (Figure 5). The vertical thickness of the thick cloud extended below and above the freezing level, with an overall thickness of around 4 km. The HID makeup of the thick cloud layer was aggregates, vertical ice, ice crystals, and wet snow, with the wet snow occurring near the freezing level. Compared to the first thick cloud case, this case had less aggregates and more ice crystals. Even though the thick cloud is much smaller in this case, the electric field is stronger, with a maximum electric field of ~600 V/m. This implies that this thick cloud is marginally electrified. Similar to the first case, higher MRR values occur near smaller electric fields, while the larger electric fields correspond to lower MRR (Figure 7). All electric field readings were positive.

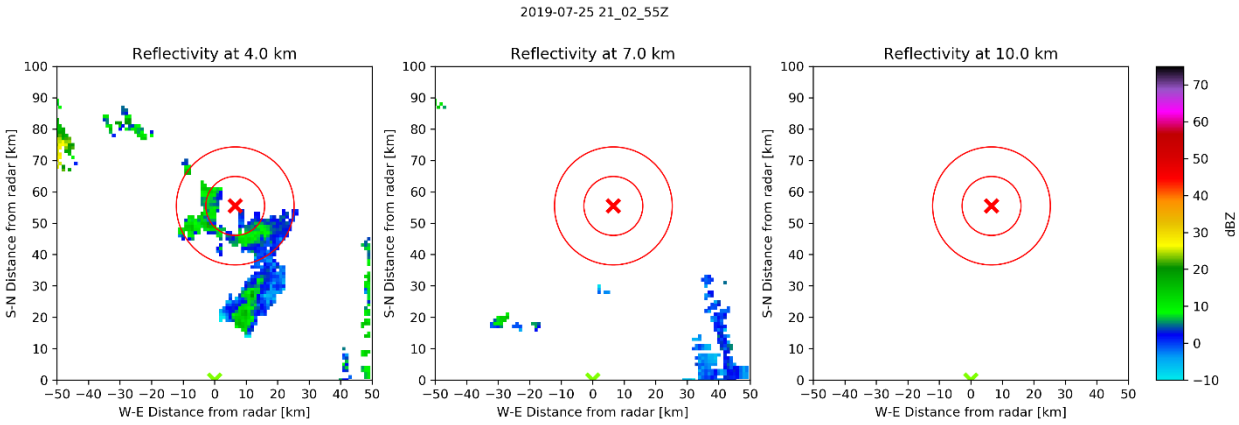

Figure 5: 4km, 7km, and 10km CAPPIs of reflectivity for a thick cloud layer from 7/25/2019.

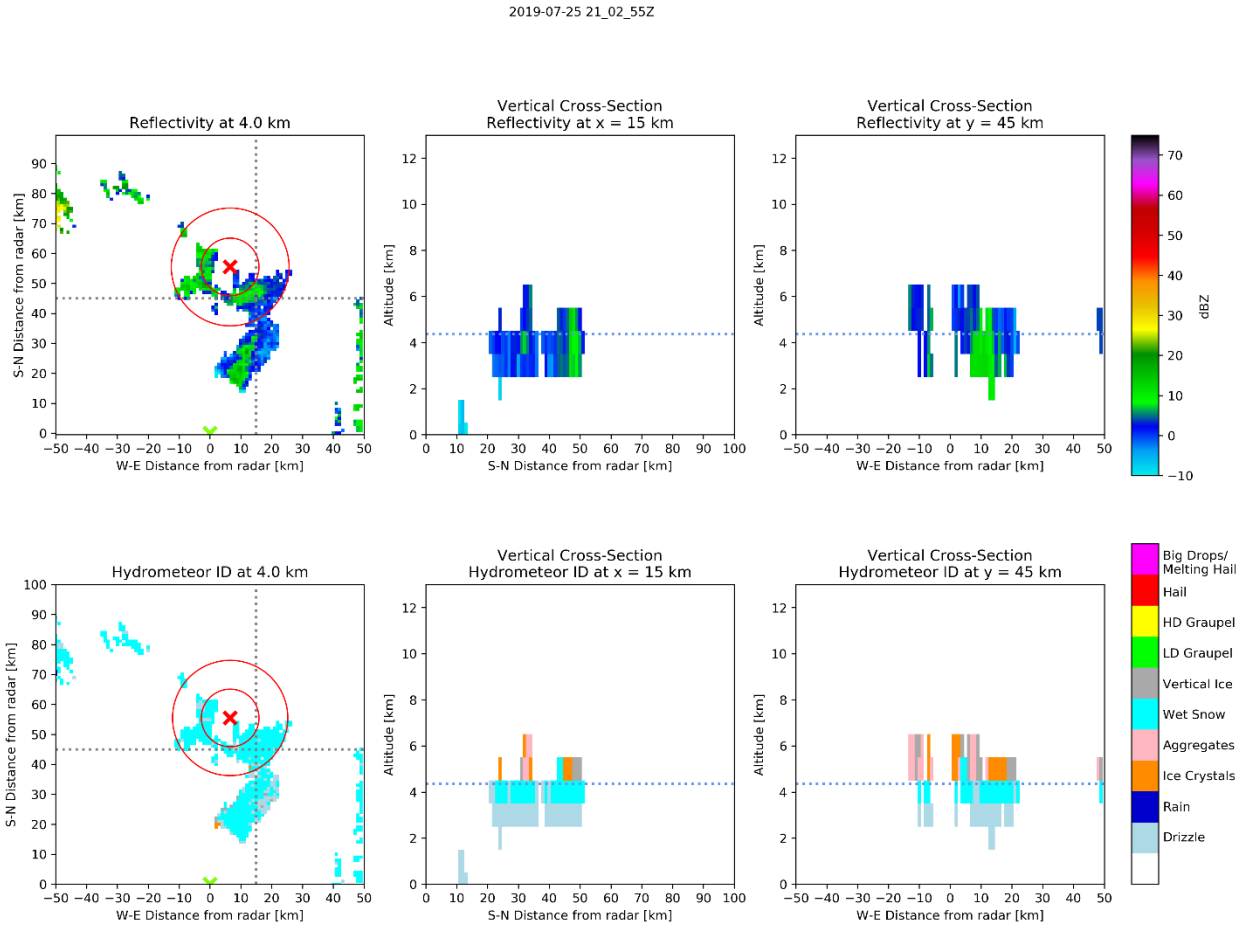

Figure 6: 4km CAPPI, and RHIs of reflectivity and HID for a thick cloud layer from 7/25/2019. Cross section location is marked by dotted lines on CAPPI and radar location is marked by the green arrow.

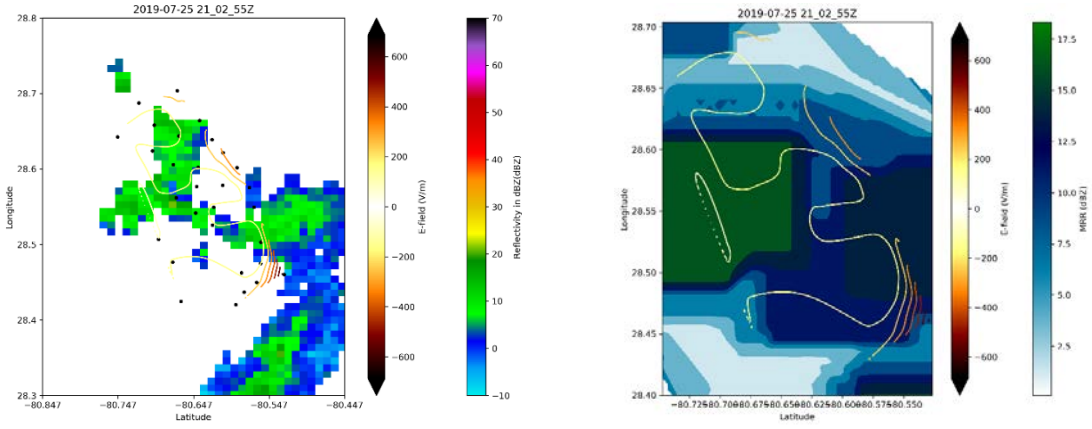

Figure 7: Electric field contours overplotted on reflectivity CAPPI (left), and MRR (right), for a thick cloud layer from 7/25/2019.

02/05/2016:

The last case is a very shallow thick cloud layer that occurred in the winter. As shown in Figure 8, reflectivity values only show up in the 7 km CAPPI, indicating the shallow nature of this cloud. The RHI plots shown in Figure 9 show the cloud is completely located above the freezing level, located between 6-9 km. HID for this thick cloud layer is composed of aggregates, vertical ice and ice crystals, with vertical ice and aggregates dominating. Electric field values are small, similar to the first case with values barely reaching above 200 V/m (Figure 10). This value is within the fair-weather field range, and even though MRR conditions were violated (>7.5 dBZ), the electric field does not point toward an electrified cloud.

Date	Approx. E-Field Maximum	Approx. MRR Maximum	Violations
2012/6/20	200	8	TC only
2013/7/19	400	35	CU and TC
2014/9/7	250	20	CU, AA, and TC
2015/1/20	250	10	TC only
2015/4/27	200	12	AA and TC
2015/12/3	300	33	DW and TC
2016/2/5	250	18	TC only
2017/3/14	800	16	DW, AA and TC
2018/11/15	150	21	TC only
2019/7/25	600	25	DW and TC
2020/6/3	200	22	TC only

Table 3: Thick cloud cases analyzed along with their maximum electric field and MRR values estimated from graphs. Violations are also logged. TC=Thick Cloud, CU=Cumulus, AA=Attached Anvil, DW=Disturbed Weather

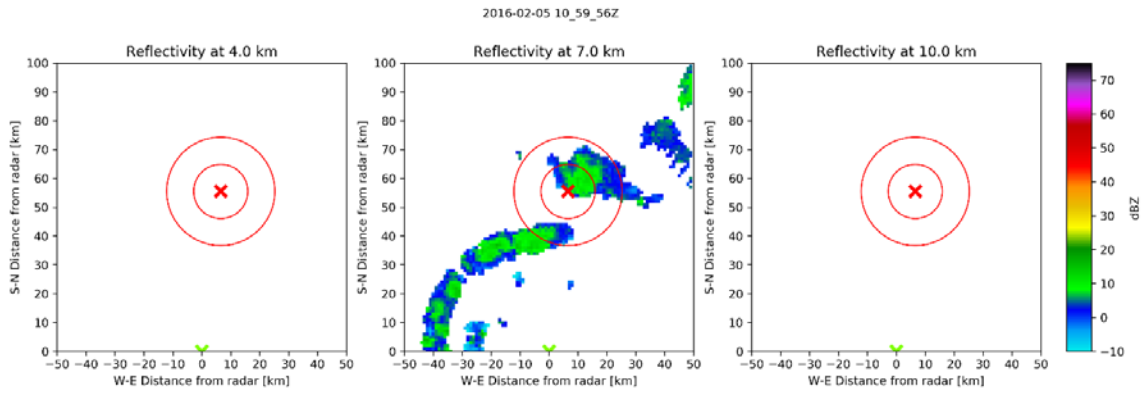

Figure 8: 4km, 7km, and 10km CAPPIs of reflectivity for a thick cloud layer from 2/5/2016.

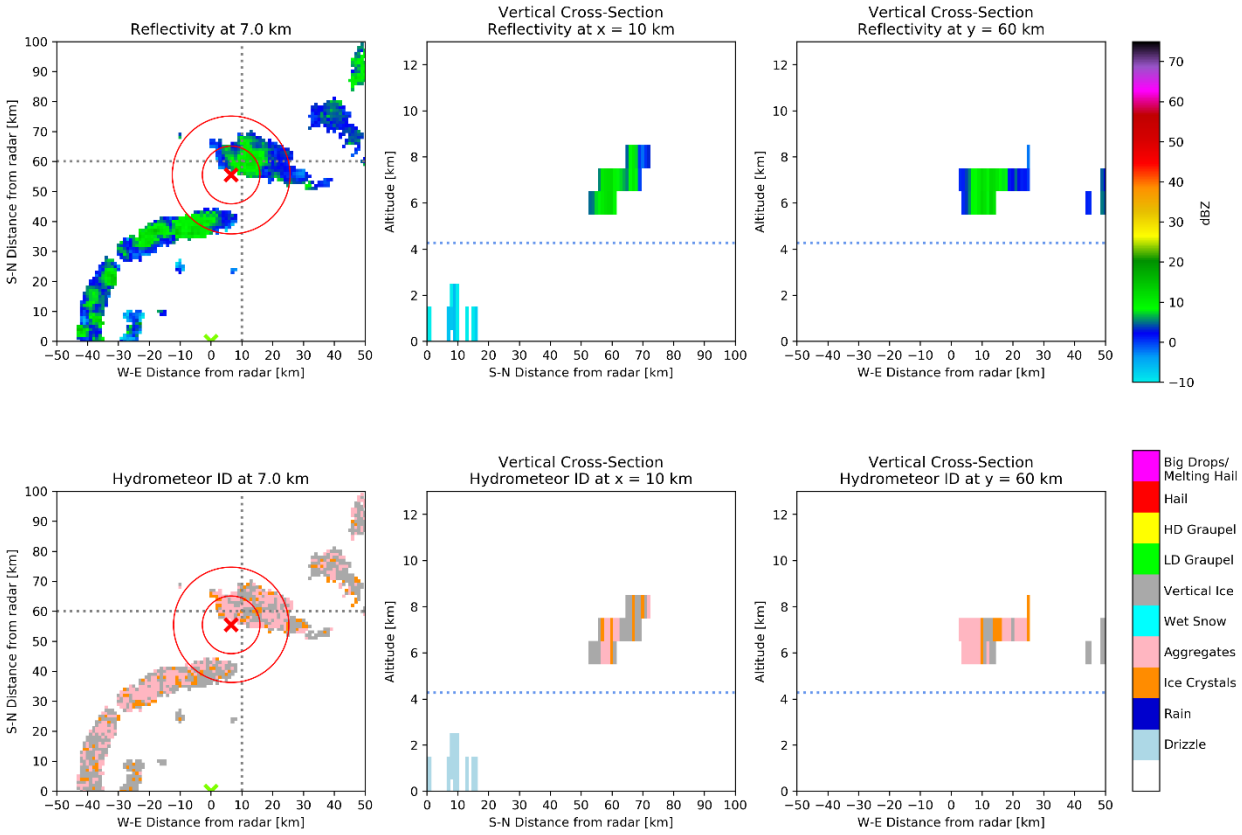

Figure 9: 4km CAPPI and RHIs of reflectivity and HID for a thick cloud layer from 2/5/2016. Cross section location is marked by dotted lines on CAPPI and radar location is marked by the green arrow.

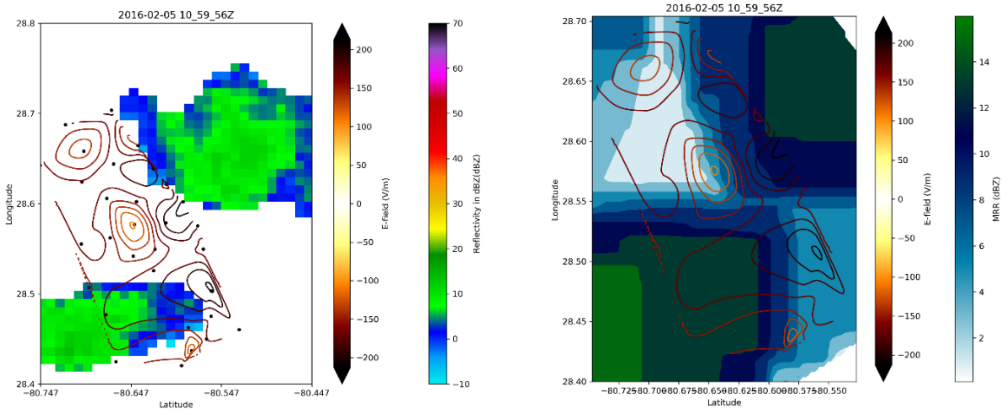

Figure 10: Electric field contours overplotted on reflectivity CAPPI (left), and MRR (right), for a thick cloud layer from 7/25/2019.

Overall Trends:

As shown in Table 3, only three out of the 11 cases analyzed had electric field values that could be considered above the fair weather field (100-300 V/m). The marginally electrified thick cloud cases all had a section of cloud below and above freezing. In theory, a cloud spanning from below freezing to above would allow for a more robust mixed phase region, which is where charging of hydrometeors is most efficient due to the presence of supercooled liquid water. Thick clouds located entirely above freezing had lower electric fields (4/27/2015 and 2/5/2016). MRR values did not show a clear pattern to stronger thick cloud electric fields. Two of the three marginally electrified clouds had MRR values higher than 25 dBZ, while the thick cloud with the highest electric field had a maximum MRR of approximately 16 dBZ. Several of the thick cloud layer cases with weak electric fields also had values above 20 dBZ. Even though all of the cases analyzed were isolated in time, there were still other violations going on before and/or after the thick cloud violations for many of the cases. All of the thick cloud cases with the highest electric fields had multiple violations occurring throughout the case day, which could affect the electric fields being measured at the surface. Case days with solely thick cloud violations had the weakest electric fields, while case days with disturbed weather and thick cloud violations had the highest electric fields. Looking at HID, marginally electrified cases had more mixture of hydrometeors, with a typical HID of 40% aggregate, 35% vertical ice, and 25% ice crystals. This result supports a more prevalent mixed phase region in marginally electrified thick clouds. Nonelectrified thick cloud cases are more likely to be dominated by a HID type. The fact that vertical ice is a dominating HID in nonelectrified clouds is puzzling and points to either an overestimation in vertical ice in the HID calculation, or the electric field mill is not picking up the fields in the thick cloud. Nonelectrified thick clouds are more likely to have higher values of VAHIRR and lower values of MRR than marginally electrified thick clouds, but have substantial overlap. This result implies that electrified thick clouds have higher reflectivity above freezing, but less of the cloud is located above freezing so the thickness above freezing is less and thus VAHIRR is less.

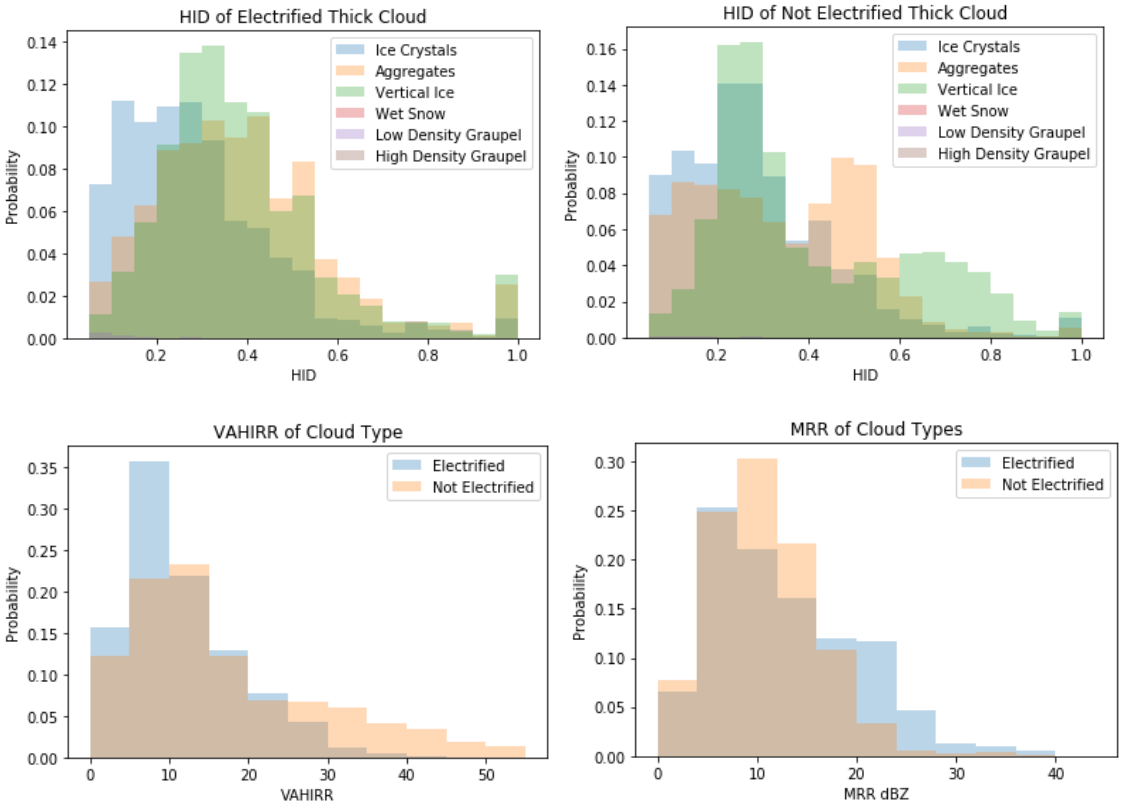

Figure 11: Radar Characteristics for marginally electrified versus nonelectrified thick clouds.

Cloud Type Characteristics

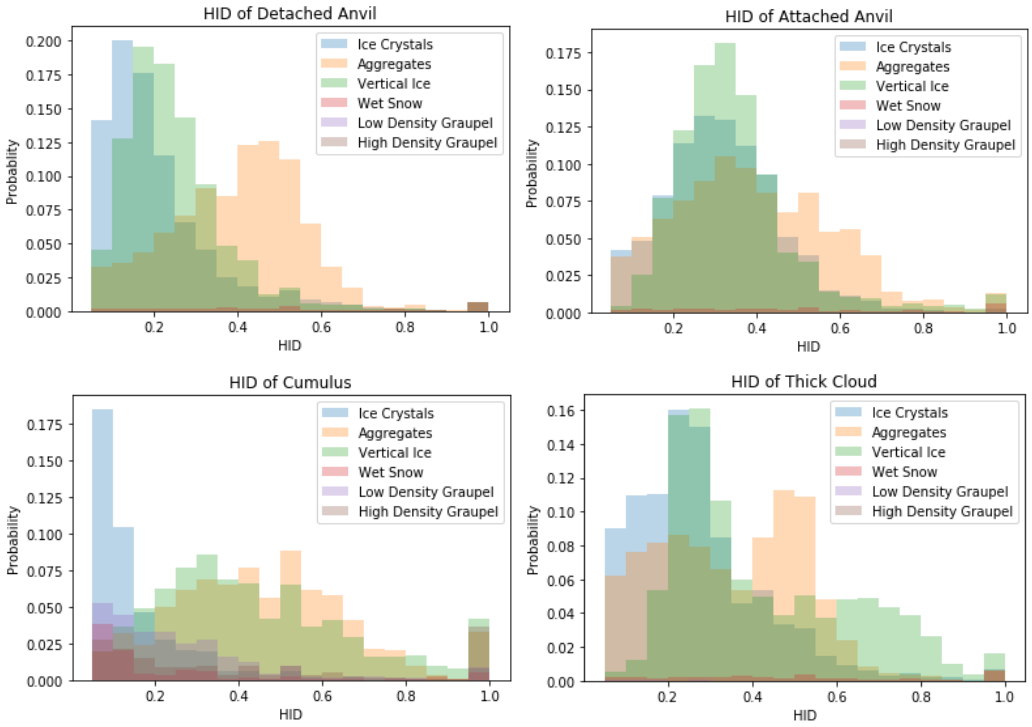

Figure 12: Histograms of HID makeup for each cloud type.

Thick Cloud HID:

For thick clouds, the most dominant HID type is vertical ice (Figure 12). This is surprising, since vertical ice is typically caused by strong electric fields orienting the ice in the vertical. When looking at our thick cloud cases, however, electric fields rarely reached even 500 V/m. This could imply that there is an overestimation in vertical ice due to the HID calculation. The second most dominant HID is aggregates, followed by ice crystals. Wet snow is minimal and low and high density graupel are nearly nonexistent in thick cloud cases.

Cumulus HID:

For cumulus, the most dominant HID types are vertical ice and aggregates. Cumulus cloud cases have the most variation in HID makeup, and the most high and low density graupel present out of cloud types. This makes sense, since cumulus clouds have the strongest updrafts of the cloud types, with updrafts able allow graupel growth to occur and be lofted above the freezing level. A typical cumulus cloud case in our data consists of approximately 50% aggregates, 30% vertical ice, 5% ice crystals, 2% low density graupel, 2% high density graupel, and 1% wet snow.

Detached Anvil HID:

The most dominant HID for detached anvils is aggregates. The distributions in Figure 12 show clear patterns, with most detached anvils being composed of approximately 50% aggregates, 30% vertical ice, and 20% ice crystals. Wet snow occurs occasionally, and high and low density graupel are minimal. Overall, the pattern present in attached anvils resembles detached anvils, with a slight shift in the distribution.

Attached Anvil HID:

The most dominant HID for attached anvils is aggregates, with vertical ice and ice crystals occurring the second most. Attached anvils have most ice crystals present out of cloud types, with most attached anvils being composed of 30% ice crystals, 30% vertical ice, and 40% aggregates. Graupel in attached anvil cases is nearly nonexistent. These values seem reasonable, since lighter particles such as ice crystals and aggregates are the most likely to be advected into the anvil from the main updraft.

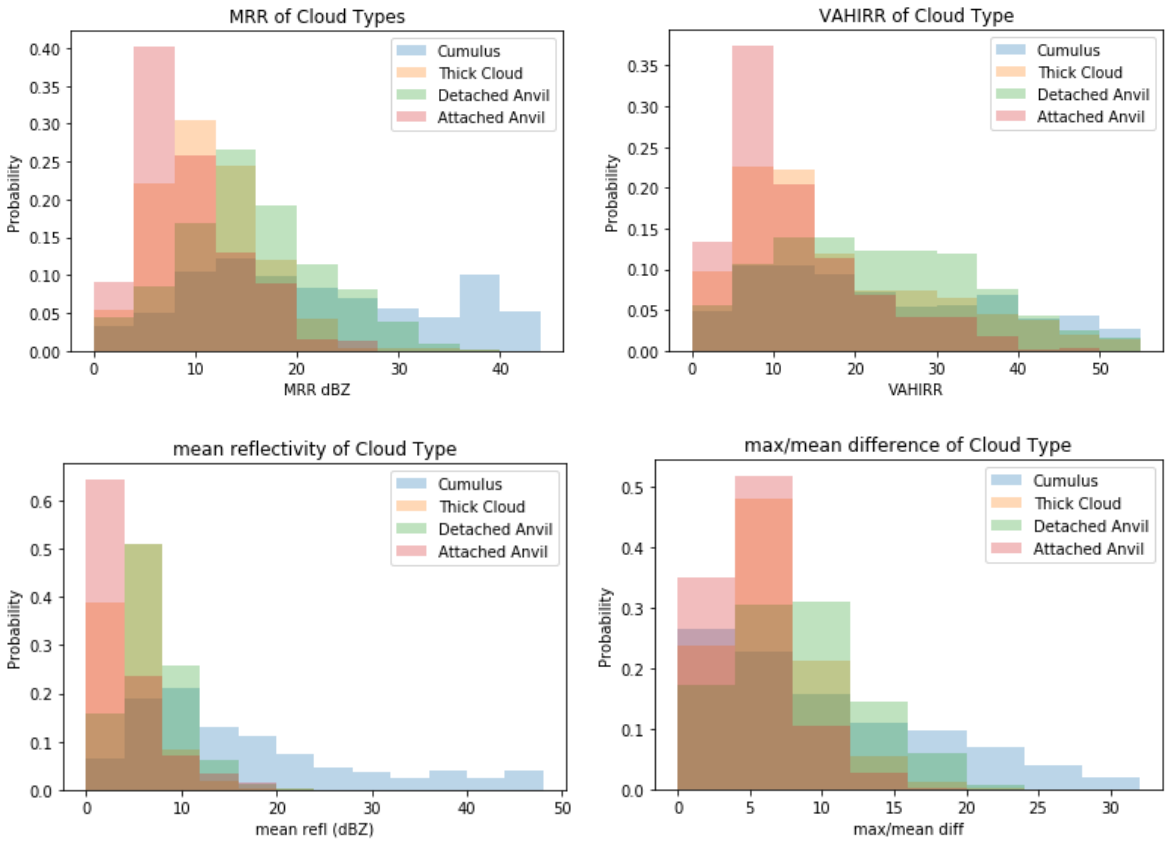

Figure 13: Histograms of reflectivity parameters for each cloud type: MRR (top left), VAHIRR (top right), mean reflectivity (bottom left), and max/mean difference (bottom right).

MRR:

Cumulus has highest MRR values followed by detached anvils. Attached anvils have the smallest MRR values, but there is substantial overlap with thick cloud MRR values. Keep in mind that MRR values in this analysis are allowed to exceed 35 dBZ.

Mean Reflectivity:

Similar to the MRR, the mean reflectivity values are highest for cumulus clouds, followed by detached anvils, and lastly attached anvils and thick clouds. Once again, attached anvil and thick cloud have substantial overlap in mean reflectivity values. This consistent overlap in variables will make distinguishing these two cloud types in the model difficult.

Max/Mean Difference:

The max/mean difference can give an idea of how cohesive a cloud is. The larger the max/mean difference, the more convective in nature a cloud will be. Looking at Figure 13, we can see that the max/mean difference trends follow most closely to the MRR trends. Cumulus have the highest max/mean difference which is reasonable since they are the most convective. Detached anvil has the second highest values, and thick cloud and attached anvil have the lowest values.

VAHIRR:

VAHIRR has overlap in all cloud types, thus probably not very useful for differentiation in the logistic regression model. Cumulus and detached anvil have the highest VAHIRR values, while thick cloud and attached anvil favor lower values.

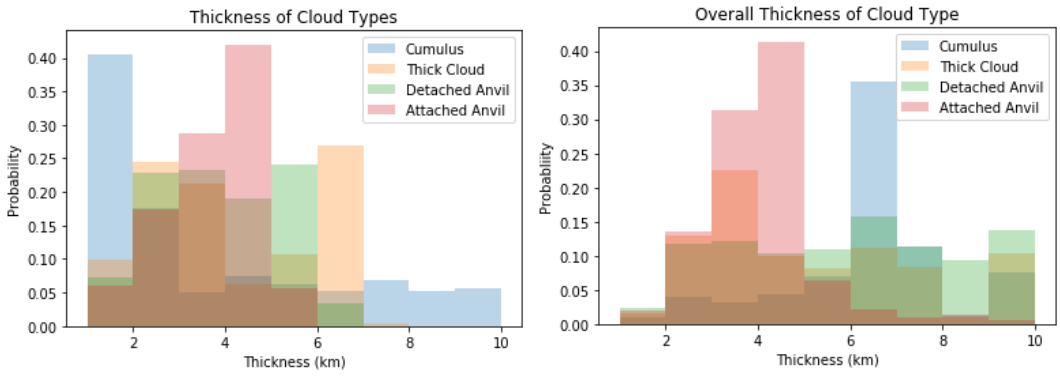

Figure 14: Histograms of thickness above the freezing level (left) and overall thickness (right) for each cloud type.

Thickness:

For thickness above the freezing level, cumulus have a large range of values (Figure 14). Most data points are located at the bottom of the distribution, but cumulus data points also compose the highest thickness values as well. Thick cloud makes up the second highest thickness averaging around 6 km. Detached and attached anvil are the least thick with values sitting between 2-5 km. When viewing the overall thickness, the distribution changes for several cloud types. Cumulus clouds are now on average thicker, with values peaking between 6-7 km. This implies that a larger portion of cumulus clouds reside below the freezing level. The attached anvil distribution stays nearly the same, peaking around 4 km. This means that attached anvils are nearly completely above the freezing level. Thick clouds are thicker when viewing overall thickness, and the distribution becomes more spread out. Thus, some thick clouds do have portions below freezing, while others do not. Detached anvil clouds also seem to become thicker when looking at overall thickness. This does not seem to match what is expected, since anvils are typically above the freezing level. Most likely, a small cloud layer lower in altitude may have made it appear that the detached anvil cloud was thicker than it actually is. Since we only have three cases of detached anvil to pull from, this artifact would be prominent. Thus, more detached anvil cases should be added to the dataset to limit data biases in the future.

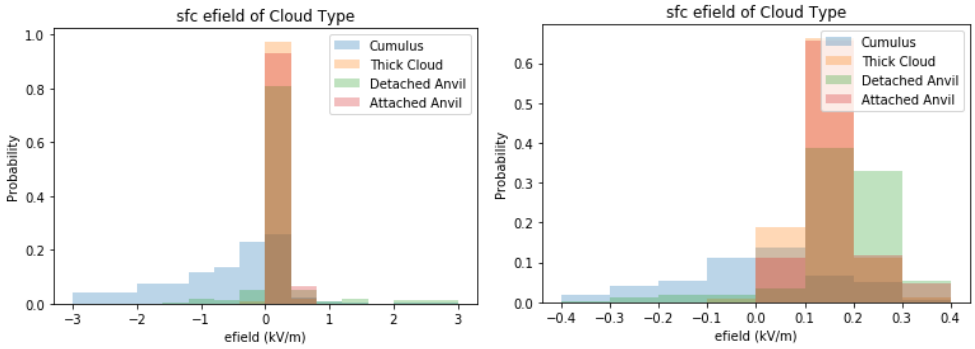

Figure 15: Histograms of the electric field (left) and a zoomed in portion of the electric field (right) to better view the smallest values for each cloud type.

Surface E-field:

The largest electric field values are associated with cumulus and detached anvil. Cumulus clouds are more likely to have a negative electric field value, while all other cloud types are associated most often with positive values. This is reasonable due to the differing nature of charge structures in the cloud. For a cumulus cloud, the negative charge layer is lower than the positive layer in the cloud, which means the electric field mill at the surface will detect the negative electric field that is shielding the positive charge layer from the sensor.

Attached and detached anvils, however, are composed mostly of positively charged ice crystals that were advected into the anvil from the convective cumulus region. Thus, the electric field mill at the surface would be most likely to detect a positive electric field underneath an anvil. Thick clouds are also associated with positive electric fields, but have very weak fields (<600 V/m). The fair-weather field is typically between 100-300 V/m, which implies that either most of the thick clouds are not electrified, or the sensor is not detecting the fields properly (this could be due to weakening of the signal as it travels to the surface if the cloud is very high).

Multinomial Logistic Regression

Collected data was input into a multinomial logistic regression model to see if it is possible to differentiate cloud type using radar characteristics and electric field mill values. Overall, the logistic regression model is able to classify 81.7% of clouds correctly. The results of the model are shown in the confusion matrix (Figure 16). Basically, values that fall in the diagonal area from the top left to bottom right were correctly predicted, while values outside of the central diagonal were incorrectly predicted. From the confusion matrix alone, we can see that most of the values fall in the middle diagonal, indicating the model did well at predicting cloud type. The category with the least predictability was attached anvil and was most often misclassified as thick cloud. This misclassification matches what was shown in our histogram analysis, with thick cloud layers and attached anvils having the most overlap in characteristics.

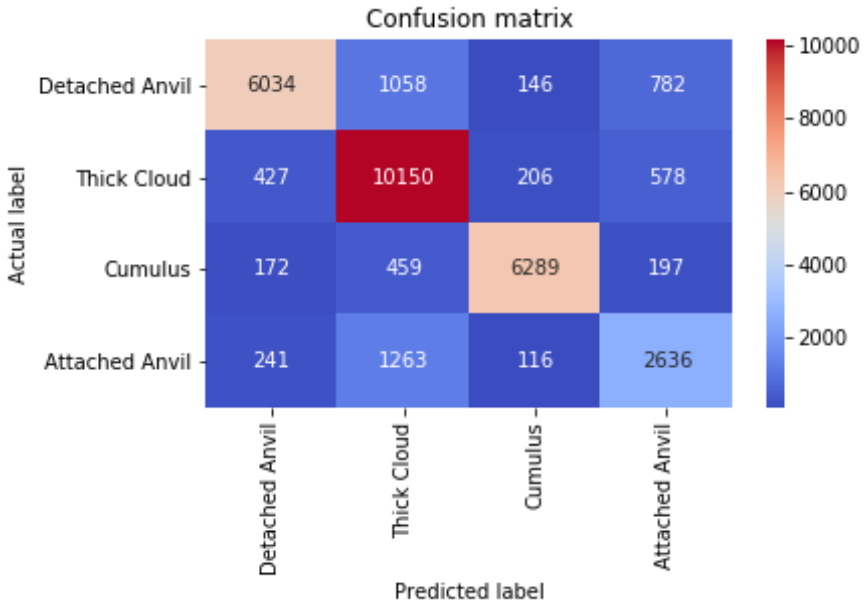

Figure 16: Confusion matrix demonstrating model performance in classifying cloud type.

Skill scores were also calculated to take a more quantitative approach in determining how well the model performed and are shown in Table 4. Overall, cumulus clouds were most accurately predicted, with a probability of detection (POD) of 93% and a false alarm ratio (FAR) of 11%. This result is understandable, since cumulus had the most unique distributions in the histograms of radar characteristics from the previous section. Detached anvil was the second best in its ability to be accurately classified, with a POD of 88% and a FAR of 25%. Thick clouds were able to be correctly classified to a moderate degree with a POD of 79% and FAR of 11%. The worst skill scores were associated with attached anvils, with a POD of 63% and FAR of 38%. More cases should be added if possible to limit data bias and variables should be tested to remove cross correlated variables. Other cloud characteristics could also be added as predictors in cloud type to better improve the model.

Type	POD	FAR
Detached	0.878	0.248
Thick	0.786	0.107
Cumulus	0.931	0.115
Attached	0.630	0.381

Table 4: Skills scores of the multinomial logistic regression for each cloud type.

Conclusion

This project researched thick cloud layer cases in depth to determine common characteristics associated with thick clouds. Cases of thick clouds and other isolated cloud types were also recorded for training purposes to see if enough differences exist between cloud types to differentiate them with an algorithm. Each case along with its corresponding characteristics was recorded in a database, and this database was used to compare differing cloud types, as well as train the algorithm to detect thick clouds. The overall takeaways from this project were:

- Most thick clouds are not electrified, or at least their electrification is not detected by the electric field mill network.
- Thick cloud cases that were marginally electrified spanned from above freezing to below, had lower VAHIRR, higher MRR, and more mixed HID than nonelectrified thick clouds, and occurred on days with multiple cloud violations.
- There is the potential to differentiate cloud type with moderate accuracy using a multinomial logistic regression, with radar characteristics as the independent variables used in prediction.
- The most useful parameters in differentiating cloud type were the HID percentages.

Future work could add new variables to the model such as cloud shape (distance in the vertical versus horizontal), dual polarization variables (KDP, ZDR, Correlation Coefficient), satellite data, as well as add many more cases into the dataset to make the results more robust. This work represents a first step in the automation of cloud type classification for the potential improvement of LLCC implementation.

Acknowledgements

I would like to thank my mentors for trusting me in this project even through switching to a remote internship. They have been so helpful and great to work with, pushing me to do great research and teaching me so much about the Lightning Launch Commit Criteria and their role in rocket launches. I would also like to thank the 45th Weather squadron for providing launch day reports and everyone I met (virtually) at KSC. You were all wonderful and I greatly enjoyed this research!

References

Christian, H. J., Mazur, V., Fisher, B. D., Ruhnke, L. H., Crouch, K., and Perala, R. P., "The Atlas/Centaur Lightning Strike Incident", J. Geophys. Res., 94(D11), 13169– 13177, 1989. doi:10.1029/JD094iD11p13169.

Dye, J. E., & Bansemer, A., "Electrification in Mesoscale Updrafts of Deep Stratiform and Anvil Clouds in Florida", Journal of Geophysical Research: Atmospheres, 124, 1021– 1049, 2019. URL: https://doi.org/10.1029/2018JD029130

Merceret, F.J., Willett, J.T., Christian, H.J., Dye, J. E., Krider, E. P., Madura, J.T., OBrien, T. P., Rust, W. D., Walterscheid, R. L., "A History of the Lightning Launch Commit Criteria and the Lightning Advisory Panel for America's Space Program", NASA/SP-2010-216283, 2010. URL: https://ntrs.nasa.gov/search.jsp?R=20110000675

Nicoll, K.A. and Harrison, R.G., "Stratiform Cloud Electrification: Comparison of Theory with Multiple In-Cloud Measurements", Q.J.R. Meteorol. Soc., 142: 2679-2691, 2016. doi:10.1002/qj.2858

Willett, J. C., and Merceret, F. J. (Eds.), Krider, E. P., Dye, J. E., O'Brien, T. P., Rust, W. D., Walterscheid, R. L., Madura, J. T., and Christian, H. J., "Rationales for the Lightning Flight-Commit Criteria", NASA/TP-2010-216291, 2017. URL: https://ntrs.nasa.gov/search.jsp?R=20170001583